

## Study of Ceria-Nickel Composites for Anode Catalytic Layer for Direct Ethanol SOFC

F. C. Fonseca<sup>a</sup>, F. N. Tabuti<sup>a</sup>, F. B. Noronha<sup>b</sup>, B. L. Augusto<sup>b</sup> and L. V. Matos<sup>c</sup>

<sup>a</sup> Instituto de Pesquisas Energéticas e Nucleares, IPEN, São Paulo, SP 05508-000, Brazil

<sup>b</sup> Instituto Nacional de Tecnologia, Rio de Janeiro, RJ 08901, Brazil

<sup>c</sup> Universidade Federal Fluminense, Niterói, RJ, 24210-240, Brazil

A hydrothermal route was used to synthesize gadolinia-doped ceria with highly dispersed Ni particles. The microstructural and electrical properties of the cermet revealed that Ni attained percolation at relatively low volume fraction. The cermet was used as a catalytic layer deposited onto the standard Ni-based anode and allowed for the stable operation under ethanol. No evidence of carbon deposits was identified after 50 hours of continuous operation under dry ethanol. Such a result was attributed to both the catalytic properties of the ceria layer and the operation mechanism of gradual internal reforming.

### Introduction

Solid oxide fuel cells (SOFC) have unique advantages such as high efficiency and fuel flexibility (1-3). The dissemination of fuel cell can be greatly boosted if readily available fuels (hydrocarbons or alcohols) can be fed directly to the SOFC, bypassing the inconveniences associated with the production, storage, and distribution of hydrogen. The conversion of such alternative fuels at the anode can be promoted due to the H<sub>2</sub> consumption by the electrochemical reaction, leading to high conversions and efficiency (1,4,5). Bio-ethanol is an attractive renewable fuel that can be obtained from different biomasses (such as sugar cane, corn, and agricultural residues), with a well-established infrastructure for both production and distribution in some countries such as USA and Brazil. The main idea is the use of a viable biofuel for the efficient and clean energy production, which does not contribute to CO<sub>2</sub> emissions, using SOFC.

The Ni/YSZ cermet is the typical anode of SOFC systems (6-8). Ni provides electronic conductivity, while YSZ provides the ionic conductivity and thermal stability. Usually, a high Ni content (at least 30 vol. %) is necessary in order to exceed the percolation threshold for electronic conductivity. However, since Ni is very active to reforming as well as cracking reactions, such a high volume fraction favors carbon deposits when hydrocarbons or bio-ethanol are used directly as the fuel in standard SOFC. The carbon deposits on metal sites of anodes, resulting in the rapid degradation of the cell performance (6,7). A significant carbon deposition has been detected on Ni/YSZ anodes of SOFC containing high Ni loading and operating directly on pure ethanol (1). Therefore, the development of anodes for SOFC running on ethanol that exhibit high catalytic activity to ethanol conversion, high stability and adequate ionic and electronic conductivity at working conditions is still a challenge.

Some strategies have been proposed for suppressing carbon deposition over SOFC anodes such as: (i) the addition of water and/or O<sub>2</sub> to the fuel; (ii) the use of redox supports, such as ceria based oxide as the ceramic phase of the anodes; (iii) the decrease of Ni content (9-14). However, it has been shown that the use of high steam/ethanol ratios decreases the electrical efficiency of the SOFC system. On the other hand, ceria-based materials are promising substitutes for zirconia-based anodes. Due to mixed ionic and electronic conductivity and high oxygen storage capacity ceria-based oxides exhibit high resistance to carbon deposition (15,16). In addition, an interesting strategy for reducing carbon deposition is to decrease the Ni content. The decrease of the metal fraction leads to the formation of smaller crystallite sizes, which are more resistant for carbon formation (17). However, cermets with metal content below 30 vol. % need high dispersion of metallic nanoparticles to achieve good performance (18,19).

In this context, the aim of the present study is to investigate Ni/CeO<sub>2</sub>:10 mol% Gd<sub>2</sub>O<sub>3</sub> (Ni/CeGd) anodes with relatively low nickel content for bio-ethanol fueled SOFC. The Ni/CeGd SOFC anodes were prepared by a hydrothermal method and the general properties were characterized aiming at the development of carbon resistant anodes for direct ethanol SOFC.

## Experimental

Gadolinium-doped ceria, CeO<sub>2</sub>:10 mol% Gd<sub>2</sub>O<sub>3</sub> (CeGd), support was synthesized by a hydrothermal method previously described (18). An aqueous solution of cerium (IV) ammonium nitrate and gadolinium nitrate was prepared with a Gd/Ce molar ratio of 1/9. Then, cerium and gadolinium hydroxides were co-precipitated by the addition of excess of ammonium hydroxide. The precipitate was transferred to an autoclave and heated to 453 K for 4 h. The precipitate was washed with distilled water and calcined at 573 K for 2 h. Ni was added to Gd/Ce support by wet impregnation using an aqueous solution of Ni(NO<sub>3</sub>)<sub>6</sub>H<sub>2</sub>O. The resulting powder was dried at 393 K and calcined at 1473 K for 5 h. Samples with Ni content in the 18 to 44 wt.% range were prepared following this procedure. In the present study, focus has been given to the sample with 18 wt.% of Ni (18 Ni/CeGd).

The synthesized materials were characterized by X-ray powder diffraction with CuK<sub>α</sub> radiation. Electrical resistance measurements of bar samples (~2x1x10 mm<sup>3</sup>) cut from pellets sintered at 1473 K were performed using four probes and a Lakeshore 370 resistance bridge. Measurements were performed upon heating/cooling at 3 K min<sup>-1</sup> from room temperature up to 1073 K.

The Ni/CeGd cermets were tested in electrolyte supported single cells. Dense yttria-stabilized zirconia (YSZ) substrates (18 mm diameter) were used for the deposition of standard Ni/YSZ anodes and La<sub>0.65</sub>Sr<sub>0.3</sub>MnO<sub>3</sub> (LSM) cathodes with a functional composite YSZ/LSM layer. The electrode layers were deposited by spin-coating, using suspensions based on terpeneol and ethyl cellulose. After the deposition of each electrode, a heat treatment for organics removal at 1073 K was followed by sintering at 1673 K and 1423 K for the anode and cathode, respectively. The Ni/CeGd catalytic layer was deposited onto the anode by spin coating followed by heat treatment at 900 °C. Au and Pt mesh current collectors were attached, using the correspondent metal ink, to the surfaces

of the anode and cathode, respectively, and cured at 1073 K. The active electrode area of single cells was  $0.78 \text{ cm}^2$ . Samples were sealed on the tip of an alumina tube with Aremco 552. Single cells tests were performed by heating the sample up to  $850 \text{ }^\circ\text{C}$  under hydrogen (3 vol.%  $\text{H}_2\text{O}$ ). Then, the fuel cell was polarized at 0.7 V and after stabilization of the system the fuel was changed to dry ethanol (32%) carried by  $\text{N}_2$ . The single cell was continuously operated while the current density ( $i$ ) at 0.7 V was monitored as a function of the operation time. Synthetic air and fuels ( $\text{H}_2$  and  $\text{N}_2$ -carried ethanol) flow rates were set to  $50 \text{ mL min}^{-1}$  by mass flow controllers and the temperature was monitored by a thermocouple placed close to the cathode side. Polarization measurements were performed using a Zahner IM6 potentiostat. SEM analyses of the fractured surfaces of the anode were carried out after fuel cell operation to examine possible carbon deposits.

## Results and discussion

X-ray diffractograms of 18Ni/CeGd showed diffraction peaks corresponding to a  $\text{Ce}_{0.9}\text{Gd}_{0.1}\text{O}_{1.95}$  (JCPDS 75-0161) and NiO (JCPDS 24018). The reduction treatment led to the appearance of diffraction peaks attributed to Ni, while NiO peaks were no longer observed. Calculated crystallite sizes using the Scherrer equation were  $\sim 40 \text{ nm}$  and  $35 \text{ nm}$  for CeGd and NiO, respectively. Such values were found to be weakly dependent on the Ni content, and the reduced reduction treatment resulted in Ni crystallite size of  $30 \text{ nm}$ .

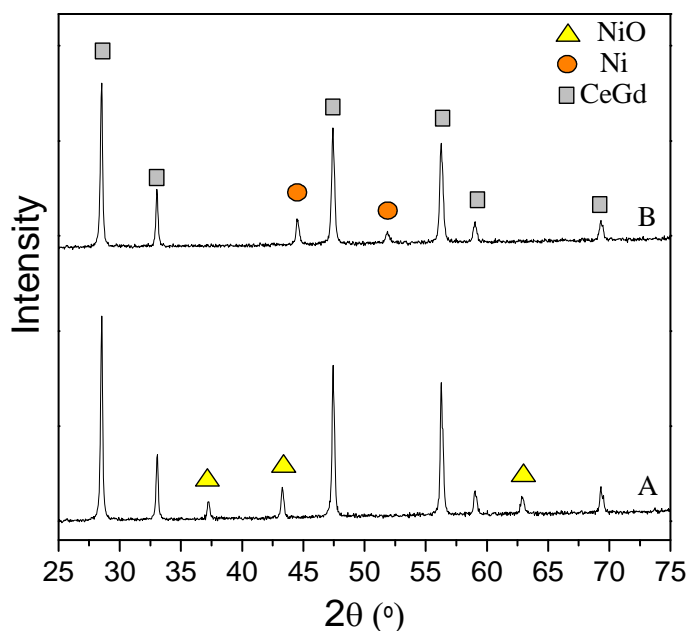


Figure 1. X-ray diffraction patterns of calcined (A) and reduced (B) Ni/CeGd samples.

The electrical properties of the Ni/CeGd catalysts were investigated over a wide temperature range. The temperature dependence of the electrical resistivity  $\rho(T)$  of sintered samples in both static air and flowing 4%  $\text{H}_2$ -Ar is shown in Fig. 2. Gadolinium-doped ceria is an oxygen ion conductor with activation energy ( $E_a$ ) values reported in the 0.6-1.0 eV interval, over a wide range of both temperature and oxygen partial pressure (20). On the other hand, NiO is a p-type semiconductor, which exhibits a discontinuity in the Arrhenius plots at a temperature close to the Néel temperature ( $T_N \sim 250^\circ\text{C}$ ) (21). The

$\rho(T)$  data in Fig 2a showed a clear slope change at  $T \sim 250$  °C in good agreement with previous reports on the electrical properties of NiO containing composites (22,23). Both low  $T$  ( $T < 250$  °C) and high  $T$  ( $T > 250$  °C) ranges were fitted according to the Arrhenius equation and calculated  $E_a$  values were 0.34 eV and 0.19 eV, respectively, in accordance with previous reports (21,24). The observed change of slope at  $T \sim T_N$  and the calculated  $E_a$  values provide strong evidences that NiO percolated in the CeGd matrix and controlled the charge transport of the composite.

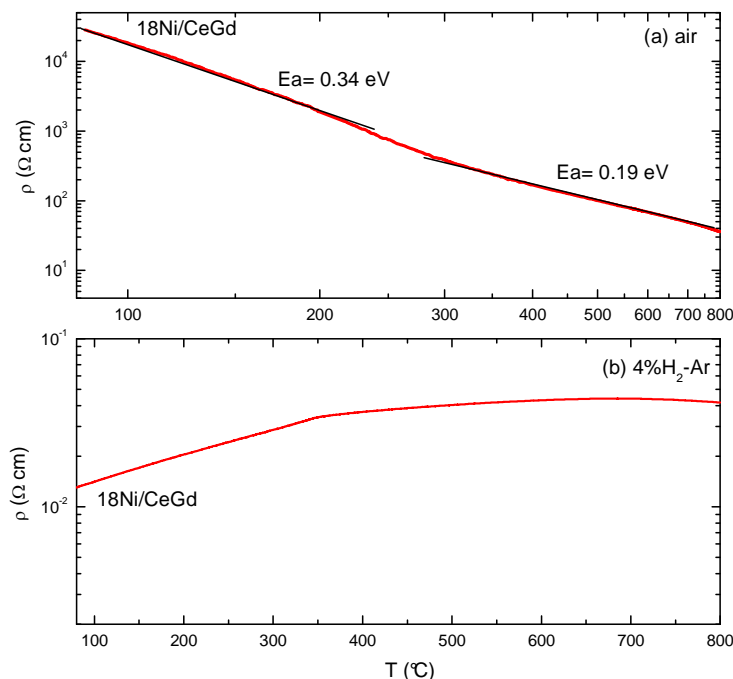


Figure 2. Temperature dependence of the electrical resistivity ( $\rho$ ) of sintered 18Ni/CeGd in (a) static air and (b) flowing 4%  $H_2$ -Ar.

Samples were reduced and  $\rho(T)$  data were recorded in flowing 4%  $H_2$ -Ar, as shown in Fig 2b. The measured  $\rho(T)$  resembled that of Ni, with a metallic behavior and a characteristic change of slope close to the Curie temperature ( $T_c \sim 350$  °C). However, as compared with Ni the magnitude of  $\rho(T)$  was shifted to higher values because of the CeGd support. Nonetheless, such a result demonstrated that Ni percolated in the composite matrix at a volume fraction of  $\sim 15$  vol.% (corresponding to 18 wt.% Ni). Such a relatively low percolation threshold may be associated with the good connectivity of Ni particles in the CeGd matrix, as well as with the average particle size ratio of the two phases. (25). However, the low Ni content resulted in relatively higher  $\rho(T)$  when compared to that of other Ni based cermets (23,26). Nevertheless, such features demonstrate that the preparation method resulted in composites with adequate microstructural properties for both catalysis and electrical transport.

As the electrical conductivity measurements indicated the percolation of relatively low volume fraction of Ni, the 18Ni/CeGd sample was added as an extra layer onto the anode. Such a layer acts as a catalyst that converts the ethanol and avoid the direct contact between the fuel and the Ni/YSZ anode (9,27-30). The current density at 0.7 V of the single cell running on dry ethanol at 850 °C was recorded as a function of time, as

shown in Fig. 3. It was observed that after stabilization during the initial hours of operation, the fuel cell exhibited remarkable stability during the tests (~50 hours) on dry ethanol. Such a result evidenced that Ni/CeGd catalyst is stable in the operation conditions of SOFCs, in agreement with previously reported catalytic studies (11).

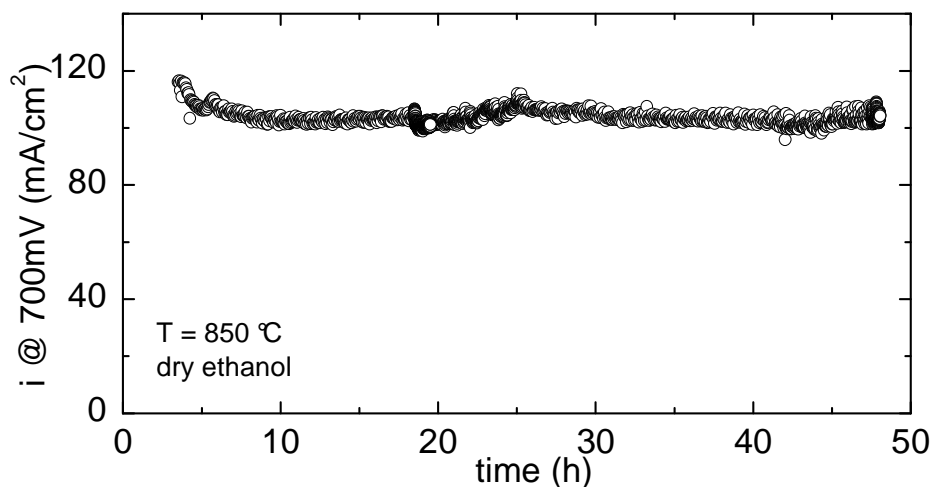
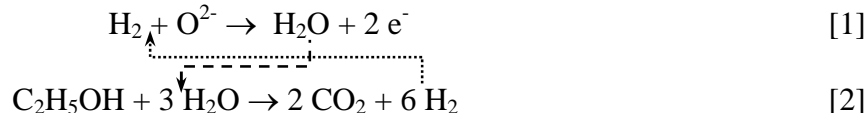


Figure 3. Time dependence of the electrical current density at 0.7 V for the fuel cell running on dry ethanol.

The good stability of the tested single cells running on anhydrous ethanol is related to the operation mechanism. Due to catalytic properties of the Ni/CeGd, the studied fuel cells operate in the gradual internal reforming of ethanol. The gradual internal reforming has been theoretically studied and experimentally demonstrated (9, 27-30). This mechanism is based on a local coupling between the steam reforming of the fuel in the catalytic layer and the hydrogen electrochemical oxidation, which takes place at the anode/electrolyte triple-phase boundary. Thus, the water released by the electrochemical oxidation of hydrogen at the anode (3) is used for the steam reforming of the ethanol (4) in the Ni/CeGd layer (27-30). Ideally, such a mechanism can be represented by the reactions:



Therefore, provided that an efficient catalyst is used, reactions [1] and [2] sustain each other and ensure stable fuel cell operation on dry ethanol as evidenced by the tests shown in Fig. 3. Usually, performance degradation due to carbon formation has been reported to be pronounced and to occur within the first minutes of operation of standard Ni-based cermets anodes fed directly with dry carbon-containing fuels (27). Therefore, fuel cell tests are in good agreement with both the catalytic properties of the ceria layer and the operation mechanism of gradual internal reforming (9,27-30).

To investigate possible carbon formation the anode of tested single cells were analyzed by SEM after the operation on ethanol. The Figure 4 shows cross section images of the anode. Differently from typical images reported in which carbon deposits

are easily detected after few hours of fuel cell operation (31), a careful analyses showed no visual evidence of carbon deposits in the anode layers of tested single cell. Such results add further evidence that the gradual internal reforming and the catalytic properties of the Ni/CeGd prevent the formation of carbon deposits in the anode of direct ethanol SOFCs.

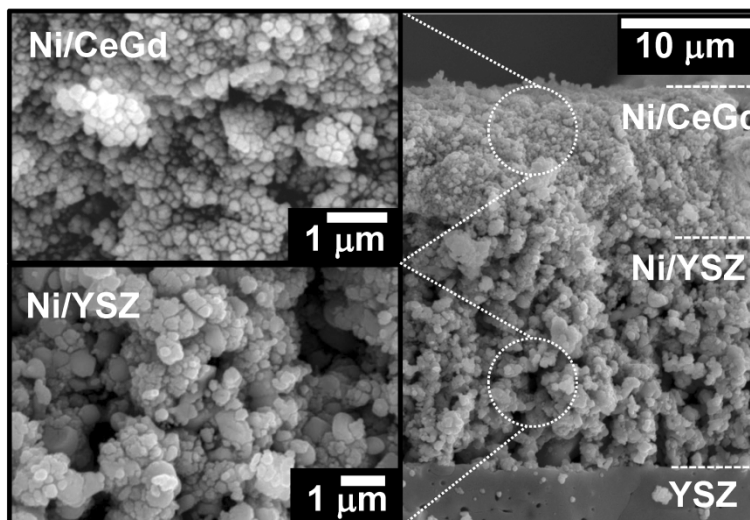


Figure 4. Scanning electron microscopy of fractured cross sections of the anode of single cells tested on direct ethanol with catalyst layer. The inset show higher magnification images of the indicated layers

### Conclusions

Ni particles were finely dispersed in co-precipitated ceria-gadolinia ceramic supports. The synthesized cermet exhibited nanometric crystallite sizes, which promoted the percolation at relatively low volume fraction (~15 vol.%) of the metallic phase, as inferred from electrical resistivity measurements. The cermet was used as an active catalytic layer deposited onto the standard Ni-cermet anode, an electrode configuration that allowed the operation with dry ethanol. The results obtained for single fuel cell operating under ethanol indicated that there is no carbon formation on Ni/CeGd anodes. This result was attributed to the catalytic properties of the ceria layer and the operation mechanism of gradual internal reforming. The present study showed that Ni/CeGd catalysts containing low Ni content are promising anode components for direct ethanol SOFCs.

### Acknowledgments

The authors are thankful for the support of the Brazilian agencies CAPES, CNPq, FINEP, CNEN, and FAPESP.

### References

1. N. Laosiripojana and S. Assabumrungrat, *J. Power Sources*, **163**, 943 (2007).

2. C. Suna and U. Stimming, *J. Power Sources*, **171**, 247 (2007).
3. P. Tsiakaras and A. Deminb, *J. Power Sources*, **102**, 210 (2001).
4. S. L. Douvartzides, F.A. Coutelieris, A.K. Demin, P.E. Tsiakaras, *Int. J. Hydrogen Energy*, **29**, 375 (2004).
5. A. Arpornwichanop, N. Chalermpanchai, Y. Patcharavorachot, S. Assabumrungrat, M. Tade, *Int. J. Hydrogen Energy*, **34**, 7780 (2009).
6. E.N. Armstrong, J. Park, N.Q. Minh, *Electrochem. Solid State Lett.*, **15**, B75 (2012).
7. R. Muccillo, E.N.S. Muccillo, F.C. Fonseca, D.Z. de Florio, *J. Electrochem. Soc.*, **155**, B232 (2008).
8. N. Q. Minh, *J. Am. Ceram. Soc.*, **76**, 563 (1993).
9. A. Atkinson, S. Barnett, R.J. Gorte, J.T.S. Irvine, A.J. Mcevoy, M. Mogensen, S.C. Singhal, J. Vohs, *Nat. Mater.*, **3**, 17 (2004).
10. S. Park, J.M. Vohs, R.J. Gorte, *Nature*, **404**, 265 (2000).
11. B.L. Augusto, L.O.O. da Costa, F.B. Noronha, R.C. Colman, L.V. Mattos, *Int. J. Hydrogen Energy*, **37**, 12258 (2012).
12. S.M. de Lima, I.O. da Cruz, G. Jacobs, B.H. Davis BH, L.V. Mattos, F.B. Noronha, *J. Catal.* **257**, 356 (2008).
13. S.M. de Lima, A.M. da Silva, L.O.O. da Costa, U.M. Graham, G. Jacobs, B.H. Davis, L.V. Mattos, F.B. Noronha, *J. Catal.*, **268**, 268 (2009).
14. X.-F. Ye, S.R. Wang, Z.R. Wang, L. Xiong, X.F. Sun, T.L. Wen, *J. Power Sources*, **177**, 419 (2008).
15. B. Huang, X. Zhu, W. Hu, Y. Wang, Q. Yu, *J Power Sources*, **195**, 3053 (2010).
16. R.A. Rocha and E.N.S. Muccillo, *Ceramica*, **47**, 219 (2001).
17. H. Song and U.S. Ozkan, *J. Catal.*, **261**, 66 (2009).
18. A.M. da Silva, K.R. de Souza, L.V. Mattos, G. Jacobs, B.H. Davis, F.B. Noronha, *Catal. Today*, **164**, 234 (2011).
19. J.R. Rostrup-Nielsen, J. Sehested, J. Norskov, *Adv. Catal.* **47**, 65 (2002).
20. V. Modafferi, G. Panzera, V. Baglio, F. Frusteri, P.L. Antonucci, *Applied Catalysis A*, **334**, 1 (2008).
21. M.W. Vernon and M.C. Lovell, *J. Phys. Chem. Solids*, **27**, 1125 (1966).
22. V. Esposito, D.Z. de Florio, F.C. Fonseca, E.N.S. Muccillo, R. Muccillo, E. Traversa, *J. Eur. Ceram Soc.*, **25**, 2637 (2005).
23. F.C. Fonseca, D.Z. de Florio, V. Esposito, E. Traversa, E.N.S. Muccillo, R. Muccillo, *J. Electrochem. Soc.*, **153**, A354 (2006).
24. V. Biju and M.A. Khadar, *J. Mater. Sci.*, **36**, 5779 (2001).
25. D.S. McLachlan, M. Blaszkiewicz, R.E. Newnham, *J. Am. Ceram. Soc.*, **73**, 2187 (1990).
26. U.P. Muecke, S. Graf, U. Rhyner, L.J. Gauckler, *Acta Materialia*, **56**, 677 (2008).
27. P. Vernoux, J. Guindet, M. Kleitz, *J. Electrochem. Soc.*, **145**, 3487 (1998).
28. J.M. Klein, S. Georges, Y. Bultel, *J. Electrochem. Soc.*, **155**, B333 (2008).
29. J.M. Klein, M. Hénault, C. Roux, Y. Bultel, S. Georges, *J. Power Sources*, **193**, 331 (2009).
30. S.D. Nobrega, M.V. Galesco, K. Girona, D.Z. de Florio, M.C. Steil, S. Georges, F.C. Fonseca, *J. Power Sources*, **213**, 156 (2012).
31. A.S. Ferlauto, D.Z. de Florio, F.C. Fonseca, V. Esposito, E. Traversa, R. Muccillo, L. O. Ladeira, *Applied Physics A, Materials Science & Processing*, **84**, 271 (2006).